

Measurements of the intrinsic torque driven by up-down asymmetric L-mode plasmas in TCV

A. Salmi¹, T. Tala¹, H. Sun², A. Jansen van Vuuren², C. F. B. Zimmermann^{3,4},
J. Ball², R. Coosemans², B. P. Duval², L. Frassinetti⁵, A. H. Karpushov²,
A. Kirjasuo¹, B. Labit², R. McDermott², O. Sauter², B. Vincent²,
the TCV team* and the EUROfusion Tokamak Exploitation Team**

¹VTT, Finland; ²EPFL, SPC, Lausanne, Switzerland; ³Max Planck Institute for Plasma Physics, Garching, Germany; ⁴Department of Applied Physics and Applied Mathematics, Columbia University, USA;

⁵KTH Royal Institute of Technology, Stockholm SE; *see author list of B.P. Duval et al 2024 Nucl. Fusion 64 112023; **see author list of E. Joffrin et al. 2024, Nuclear Fusion 64 112019

Introduction

Toroidal rotation in tokamak plasmas is beneficial for stabilizing magnetohydrodynamic (MHD) instabilities, such as neoclassical tearing modes (NTMs) and resistive wall modes (RWMs), and suppressing turbulence to enhance confinement. While neutral beam injection (NBI) efficiently induces rotation in current devices, reactor-scale plasmas require alternative momentum sources due to diminished effectiveness at higher densities and larger scales. Intrinsic rotation generated by plasma asymmetries thus becomes critical.

Previous studies at TCV have examined intrinsic rotation driven by up-down asymmetric equilibrium shapes in Ohmic plasmas [1]. Here, we extend these studies to neutral beam (NB)-heated L-mode plasmas, quantifying intrinsic torque via balanced NBI experiments.

Experimental Setup

Experiments utilized TCV's balanced NBI system to achieve near-zero rotation plasmas, minimizing momentum transport effects. The plasma current (233 kA) was counter-clockwise (top view) with co- and counter-clockwise toroidal magnetic fields (± 1.44 T). Both positive and negative up-down asymmetric shapes were investigated. Figure 1 illustrates the shapes achieved and the evolution of the toroidal angular frequency of Carbon⁶⁺, assumed to represent the main ion rotation, is measured with the charge exchange spectroscopy (CXs). The intrinsic torque can be estimated for each time slice but is least influenced by the momentum transport fluxes near the time of rotation reversal when both the rotation and rotation gradients are smallest. The rate of rotation changes outside mid radius are slow enough to ignore.

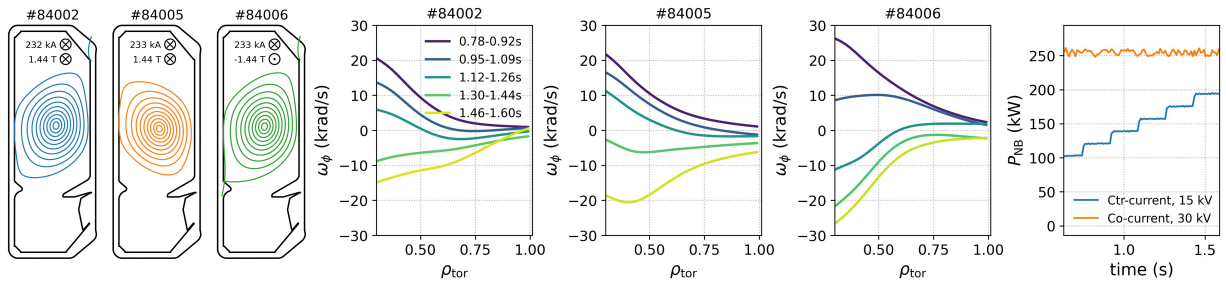


Figure 1 (Left) Up-down asymmetric shapes and toroidal magnetic field and current directions; (middle) toroidal rotation profile evolution throughout the NB torque/power ramp; (right) NB injection powers for the co- and counter-current directed beams. q_{95} values are 3.8, 3.3 and -4.2 for the discharges 84002, 84005 and 84006, respectively.

These plasmas exhibited sawtooth instabilities (~ 190 Hz), primarily affecting the core with minimal impact outside the inversion radius $\rho_{tor} \sim 0.35$ which also marks the innermost radius of the CXs measurements due to slightly up-shifted equilibria. Despite engineering

matches, slight variations in plasma volume, kinetic profiles, and consequently q_{95} (see Figure 1 caption) necessitated careful analysis and simulations that accounted for all changes.

Figure 2 compares key parameters for the discharges near their minimum rotation phase (torque step 3 for #84002 and #84005, and step 2 for #84006). The slight differences in plasma volume and density for #84006 are reflected in the local neutral beam torque density as well.

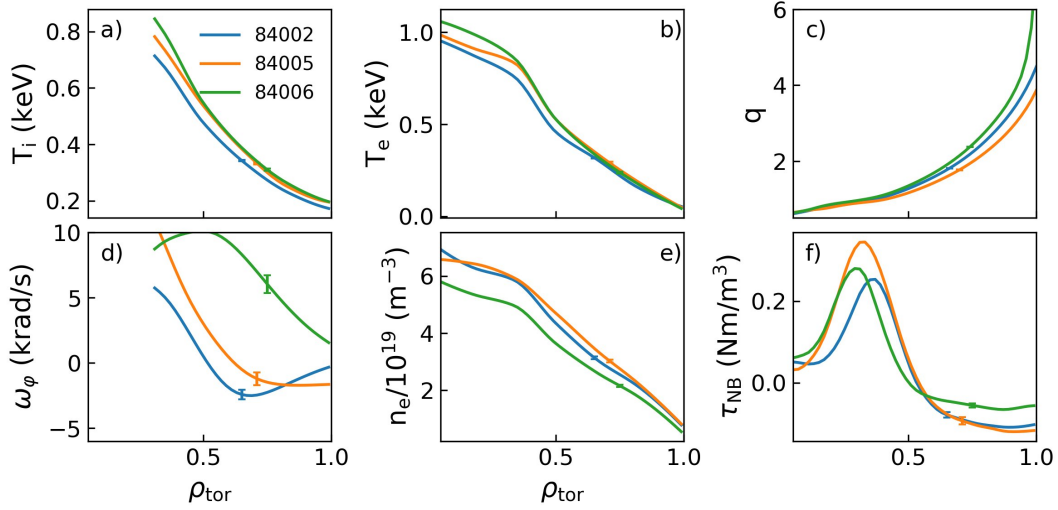


Figure 2 . Comparison of kinetic profiles (a,b,d,e), safety factor (c), and TRANSP-evaluated net neutral beam torque (f) at the time of minimum rotation, just before core sign reversal. All quantities are averaged over the corresponding time step (~140 ms). Error bars indicate one standard deviation during this interval.

Analysis Methodology

Intrinsic torque τ_{int} estimation technique follows that of [2] with the exception that the momentum transport coefficients are now estimated with gradient driven non-linear gyrokinetic GENE simulations.

$$\int V' \tau_{\text{int}} d\rho = -mnRV' \langle (\nabla\rho)^2 \rangle \left(\chi_\phi \frac{\partial v_\phi}{\partial \rho} - V_c v_\phi \right) - \int V' \tau_{\text{NB}} d\rho \quad (1)$$

Here, the magnetic equilibrium quantities $\langle (\nabla\rho)^2 \rangle$ and $V' = \partial V / \partial \rho$, as well as the neutral beam driven torque τ_{NB} , are evaluated using TRANSP. The density n and toroidal rotation v_ϕ are measured by Thomson scattering and charge exchange spectroscopy (CXs) diagnostics. The diffusive (χ_ϕ) and convective (V_c) momentum transport coefficients are obtained using the turbulent ion heat diffusion χ_i inferred via power balance from experimental data, together with the Prandtl number Pr and pinch coefficient Pn evaluated by GENE, such that $\chi_\phi = \text{Pr} \cdot \chi_i$ and $V_c = -\text{Pn} \cdot \chi_\phi / R_0$. For plot labels, we use the shorthand notation: $T_{\text{int}} = -T_{\text{diff}} - T_{\text{conv}} - T_{\text{NB}}$.

These non-linear local GENE simulations capture the ballooning mode spectrum that arises from asymmetric flux surfaces and can be used to estimate Prandtl number and pinch coefficient relatively accurately. For the calculation of intrinsic torque, these simulations neglected higher order terms such as profile shearing. These are not included in the present analysis due to currently prohibitive computational demands. The local flux-tube simulations were performed using a general Miller geometry reconstructed from experimental equilibrium and other plasma parameters at $\rho_{\text{tor}} = 0.4, 0.6, 0.8, 0.9$. Linear scans indicated that ion-scale ITG and TEM turbulence dominate, while ETG modes are subdominant and were therefore excluded from the non-linear runs. Figure 3 shows the TGLF scan, which supports this

assessment. Carbon impurities (5.47–6.6% in density) significantly reduced linear growth rates, justifying their inclusion in the non-linear simulations. Each simulation was evolved to a stationary state $t > 150 R_0/c_s$, from which ion heat and momentum fluxes were extracted. The Prandtl number and momentum-pinch coefficient were calculated using the standard approach, based on additional runs in which rotation and/or its gradient were suppressed.

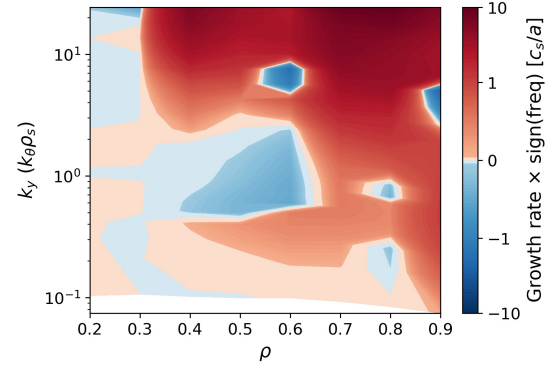


Figure 3. OMFIT/TGLF linear growth rate of the fastest growing mode with experimental parameters for #84002. Red color indicates TEM and blue color ITG.

Results

The inferred intrinsic torque estimated using Eq.(1) for TCV discharge #84002 is shown in Figure 4, alongside the contributions from other torque components. The intrinsic torque profile found is predominantly counter-current in the core and co-current at the edge broadly compensating the net NB torque at low absolute toroidal rotation. The corrections from momentum transport fluxes and transient effects are not dominating.

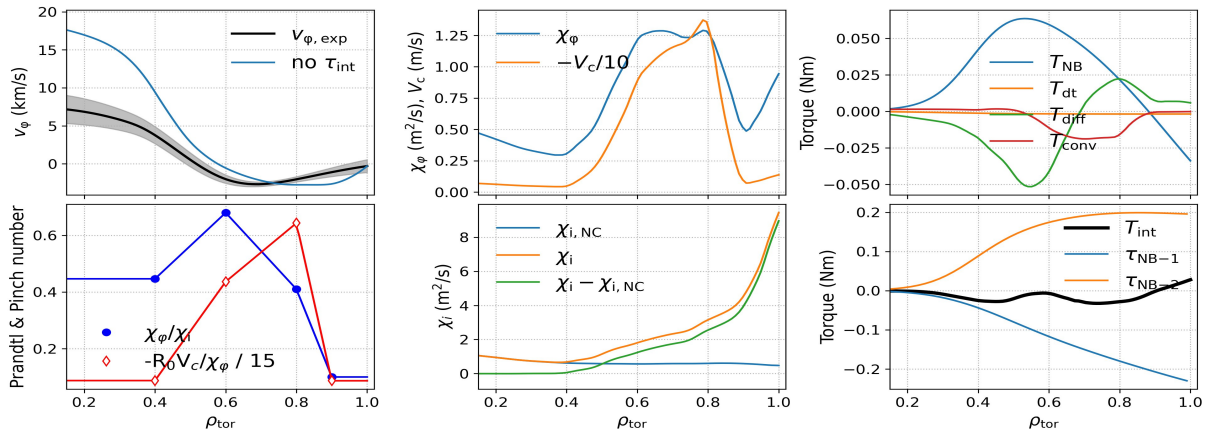


Figure 4. Intrinsic torque analysis for #84002. (left) experimental toroidal rotation v predicted rotation with τ_{int} ignored, and GENE estimated Prandtl number and momentum-pinch coefficient; (middle) turbulent ion heat conductivity from power balance with neo-classical heat diffusion subtracted (TRANSP), and the resulting momentum diffusion and convection; (right) volume integrated torque components: net NB torque, transient, diffusive, convective, NB-1, NB-2 and the resulting total intrinsic torque.

Figure 5 presents the intrinsic torque analysis for discharge #84002 across the full torque ramp. It demonstrates that intrinsic torque can be reasonably estimated outside the null rotation region, provided that transport is approximately known. Despite substantial changes in rotation and its gradient, including sign reversals, the intrinsic torque estimate remains relatively stable. This

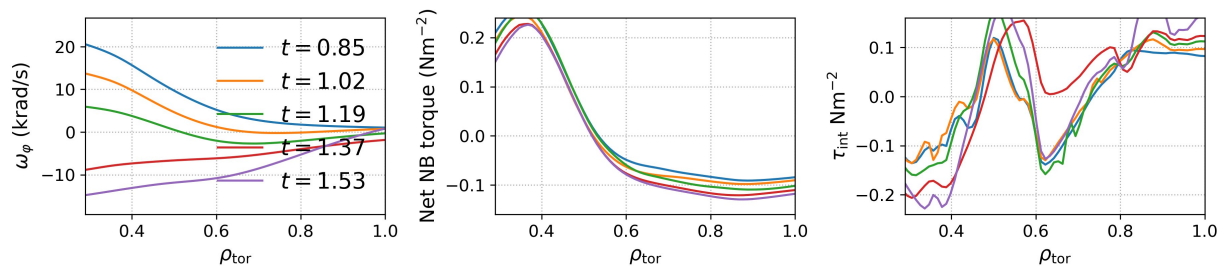


Figure 5. Intrinsic torque analysis for #84002 throughout the torque ramp. (left) toroidal angular frequency; (middle) net NB torque; (right) intrinsic torque density.

suggests that intrinsic torque can be inferred even in regimes where rotation is small but does not cross zero, enabling studies over broader parameter ranges.

Figure 6 compares the experimentally inferred intrinsic torque profiles both in torque density and as volume integrated torques. The right-hand side plots show both the GENE-estimated up-down asymmetry intrinsic torque and the experimental intrinsic torque (dashed lines), with the central plasma contribution removed such that $T_{\text{int,exp}}(\rho_{\text{tor}} = 0.4) = 0$. Apart from the outermost point for 82005 GENE estimates are close to the experimental values.

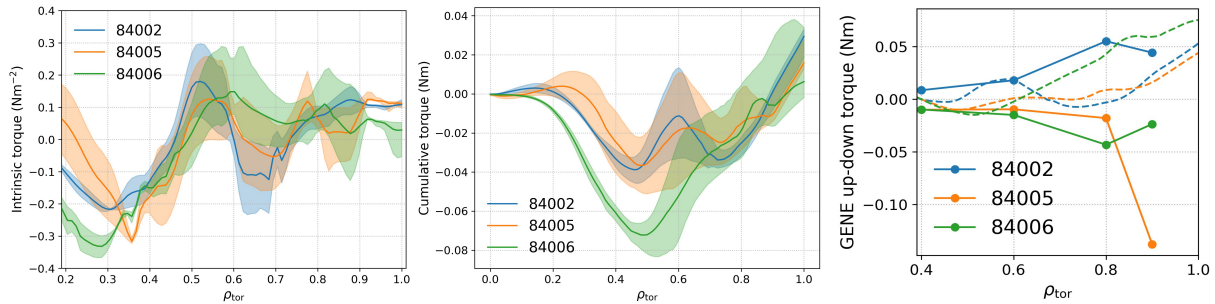


Figure 6. (Left) Intrinsic torque density; (middle) cumulative intrinsic torque; (right) comparison between GENE-predicted up-down asymmetry torque and the experimentally inferred intrinsic torque (dashed lines), excluding contributions from inside $\rho_{\text{tor}} = 0.4$ (dashed lines). The 1σ confidence bounds are derived from 1000 Monte Carlo samples of rotation profiles, assuming 50% relative uncertainty in the Prandtl numbers and momentum pinch coefficients.

However, the experimental estimates also include other intrinsic torque sources and potentially unaccounted contributions, making direct comparison difficult. This is also evident from the fact that the experimental data remains fully co-current at outer radii, even though a sign change is expected when either the plasma shape or the toroidal field is flipped [1]. The positive torque offset appears to be on the order of 0.05 Nm, or approximately 20% of the torque from a single NB unit.

Summary and Outlook

This study successfully quantified intrinsic torque in up-down asymmetric NB-heated L-mode plasmas at TCV tokamak. Counter-current intrinsic torque dominated the plasma core, while edge regions exhibited significant co-current contributions consistent with DIII-D results [5]. Non-linear local GENE simulations of up-down asymmetry intrinsic torque are of similar magnitude as inferred from experiments but overall uncertainties still leave room for other intrinsic torque sources such as profile, $E \times B$, or turbulence intensity shearing [6]. Future experiments will refine shape and profile matches and explore new parameter ranges. Ultimately, these findings contribute to understanding intrinsic rotation generation, essential for predicting and optimizing reactor-scale plasma performance.

References

- [1] Y. Camenen et al 2010 PPCF 52 12437 [2] A. Salmi et al 2024, EPS conference, P4.059
 [3] C. F. B. Zimmerman et al 2024 PoP 31 042306 [4] H. Sun et al 2024 Nucl. Fusion 64 036026
 [5] W.M. Solomon et al 2011 Nucl. Fusion 51 073010 [6] P.H. Diamond et al 2009 Nucl. Fusion 49 045002

This work has been carried out within the framework of the EUROfusion Consortium, partially funded by the European Union via the Euratom Research and Training Programme (Grant Agreement No 101052200 — EUROfusion). The Swiss contribution to this work has been funded by the Swiss State Secretariat for Education, Research and Innovation (SERI). Views and opinions expressed are however those of the author(s) only and do not necessarily reflect those of the European Union, the European Commission or SERI. Neither the European Union nor the European Commission nor SERI can be held responsible for them.